

## EXTREME SUPERNOVA MODELS FOR THE SUPERLUMINOUS TRANSIENT ASASSN–15lh

E. CHATZOPOULOS<sup>1,7</sup>, J. C. WHEELER<sup>2</sup>, J. VINKO<sup>2,3,4</sup>, A. P. NAGY<sup>3</sup>, B. K. WIGGINS<sup>5,6</sup>, AND W. P. EVEN<sup>5</sup>

<sup>1</sup>Department of Astronomy & Astrophysics, Flash Center for Computational Science, University of Chicago, Chicago, IL, 60637, USA

<sup>2</sup>Department of Astronomy, University of Texas at Austin, Austin, TX, 78712, USA

<sup>3</sup>Department of Optics and Quantum Electronics, University of Szeged, Dóm tér 9, Szeged, 6720 Hungary

<sup>4</sup>Konkoly Observatory, Research Centre for Astronomy and Earth Sciences, Hungarian Academy of Sciences, P.O. Box 67, H–1525, Budapest, Hungary

<sup>5</sup>Center for Theoretical Astrophysics/CCS–2, Los Alamos National Laboratory, Los Alamos, NM, 87544, USA

<sup>6</sup>Brigham Young University, Department of Physics and Astronomy, Provo, UT, 84602, USA

Submitted to ApJ on 2016 March 22

### ABSTRACT

The recent discovery of the unprecedentedly superluminous transient ASASSN–15lh (or SN 2015L) with its UV–bright secondary peak challenges all the power–input models that have been proposed for superluminous supernovae. Here we examine some of the few viable interpretations of ASASSN–15lh in the context of a stellar explosion, involving combinations of one or more power inputs. We model the lightcurve of ASASSN–15lh with a hybrid model that includes contributions from magnetar spin–down energy and hydrogen–poor circumstellar interaction. We also investigate models of pure circumstellar interaction with a massive hydrogen–deficient shell and discuss the lack of interaction features in the observed spectra. We find that, as a supernova ASASSN–15lh can be best modeled by the energetic core–collapse of a  $\sim 40 M_{\odot}$  star interacting with a hydrogen–poor shell of  $\sim 20 M_{\odot}$ . The circumstellar shell and progenitor mass are consistent with a rapidly rotating pulsational pair–instability supernova progenitor as required for strong interaction following the final supernova explosion. Additional energy injection by a magnetar with initial period of 1–2 ms and magnetic field of  $0.1–1 \times 10^{14}$  G may supply the excess luminosity required to overcome the deficit in single–component models, but this requires more fine–tuning and extreme parameters for the magnetar, as well as the assumption of efficient conversion of magnetar energy into radiation. We thus favor a single–input model where the reverse shock formed in a strong SN ejecta – CSM interaction following a very powerful core–collapse SN explosion can supply the luminosity needed to reproduce the late–time UV–bright plateau.

*Keywords:* supernovae: general – circumstellar matter – stars: evolution – stars: mass–loss – stars: massive

### 1. INTRODUCTION

Contemporary unbiased, large field of view, rapid–cadence transient searches have yielded the spectacular discoveries of more than a hundred superluminous supernovae (SLSNe) over the past 11 years (Quimby et al. 2007; Smith et al. 2007; Gal–Yam 2012; Chatzopoulos et al. 2013b; Nicholl et al. 2014). These ultra–bright stellar explosions exhibit a large degree of diversity both in terms of their observed light–curves (LCs) and spectra (Gal–Yam 2012; Nicholl et al. 2015). Typically, SLSNe reach peak luminosities in excess of absolute V–magnitude ( $M_V$ )  $-21$  mag and their light–curve evolution timescales vary from very fast (rise time to peak luminosity,  $t_{\text{rise}} \simeq 1–2$  weeks) to very slow ( $t_{\text{rise}} > 100$  d) (Gal–Yam 2012; Nicholl et al. 2016). The late–time decline rates of SLSN LCs also vary, with only a handful being consistent with the radioactive decays of  $^{56}\text{Ni}$  and  $^{56}\text{Co}$ , a mechanism that is known to power hydrogen–deficient (Type Ib/c) core–collapse supernova (CCSN) and thermonuclear Type Ia SN events. The spectra of SLSNe are also diverse with some events exhibiting clear signs of hydrogen–rich (H–rich) SN ejecta–circumstellar matter (CSM) interaction (SLSN–II) and the presence of strong H emission features (Gal–Yam 2012), and others lacking hydrogen and even helium with spectra often similar to Type Ic SNe (SLSN–I; Quimby et al. 2011). The host galaxy environments of most SLSNe, especially SLSN–I, are associated with low–metallicity, faint dwarf galaxies, in many cases similar to those of Gamma–Ray Bursts (GRBs) (Neill et al. 2011; Lunnan et al. 2014; Leloudas et al. 2015).

The extraordinary luminosities of SLSNe can, in principle, be provided by three different power–input mechanisms: the radioactive decay of large quantities of newly synthesized  $^{56}\text{Ni}$  ( $M_{\text{Ni}} > 10 M_{\odot}$ ) in the context of pair–instability supernovae (PISNe) (Heger & Woosley 2002; Nomoto et al. 2007; Kasen et al. 2011; Dessart et al. 2013; Kozyreva et al. 2014a,b; Kozyreva & Blinnikov 2015; Chatzopoulos et al. 2015), energy injection by a rapidly spinning newly–born magnetar (Ostriker et al. 1972; Shklovskii 1976; Kasen & Bildsten 2010; Woosley 2010; Dessart et al. 2012; Inserra et al. 2013; Metzger et al. 2015; Nicholl et al. 2015; Sukhbold & Woosley 2016; Nicholl et al. 2016) and shock heating due to the interaction of SN ejecta with a dense CSM shell (Grasberg & Nadezhin 1986; Chevalier & Fransson 1994; Smith et al. 2007; Woosley et al. 2007; Chatzopoulos et al. 2011; Chatzopoulos & Wheeler 2012b; Moriya & Tominaga 2012; Moriya et al. 2013; Chatzopoulos et al. 2013b; Dessart et al. 2015), see also (Smith & McCray 2007) and subsequent discussion in (Moriya et al. 2013).

The CSM interaction mechanism is widely accepted for the vast majority of SLSN–II due to the observed intermediate–width Balmer emission lines in the optical spectra of these events. As such, the spectroscopic properties of SLSN–II are reminiscent of those of their lower–luminosity SN II in counterparts, but the nature of the underlying explosion remains unknown. On the contrary, the origin of SLSN–I remains largely a mystery; some members of this class have been proposed as PISN candidates (Gal–Yam et al. 2009), while others have been associated with magnetar spin–down models (Inserra et al. 2013; Nicholl et al. 2015; Sukhbold & Woosley

<sup>7</sup> Enrico Fermi Fellow; manolis@flash.uchicago.edu

2016). The possibility of H-poor CSM interaction for SLSN-I is debated due to the lack of emission lines in the spectra, but cannot be totally ruled out until a deeper understanding of the metallic (non H or He) line formation processes are clarified via numerical calculations. Plausible arguments have been made on the conditions necessary to produce or suppress interaction features in the spectra of hydrogen-deficient events (Chatzopoulos et al. 2012; Chatzopoulos & Wheeler 2012b; Chatzopoulos et al. 2013b; Dessart et al. 2016).

The recent intriguing discovery of the H-poor superluminous transient ASASSN-15lh, or SN 2015L, reaching peak bolometric luminosity of  $L_{\text{bol,peak}} = 2.2 \times 10^{45} \text{ erg s}^{-1}$  has severely strained the above-mentioned power-input mechanisms, thus questioning its SN origin (Dong et al. 2016). If this event is indeed a SN, it would be the most luminous SN discovered to date. In this paper, we examine the few viable models of ASASSN-15lh in the context of an energetic stellar explosion of a massive star invoking multiple power input mechanisms.

Our paper is organized as follows. In § 2 we assess the observed properties of ASASSN-15lh, namely the early bright LC and late-time UV-bright plateau (Brown et al. 2016) and discuss the progenitor models presented in the literature up to now. In § 3 we present model fits to the full observed bolometric LC of ASASSN-15lh for single and combined power-inputs involving a rapidly-rotating pulsational PISN progenitor. Finally, in § 4 we summarize our results and discuss our conclusions.

## 2. ASASSN-15lh: THE MOST LUMINOUS EXPLOSION

### 2.1. Early observations (< 100 days).

ASASSN-15lh was discovered on 14 June 2015 (UT) by the All-Sky Automated Survey for SuperNovae (ASAS-SN; Shappee et al. 2014) at a position coincident with a bright ( $M_K \simeq -25.5$ ) host galaxy with low star-formation rate (SFR) and redshift  $z = 0.2326$  corresponding to a luminosity distance of 1171 Mpc assuming the cosmological parameters from the Planck mission (Planck collaboration; Planck Collaboration et al. 2014) as adopted also by Dong et al. (2016). The transient reached a peak absolute AB magnitude of  $M_{u,AB} = -23.5$  over a time-scale of  $\simeq 25$  d at the rest-frame making it the brightest SLSN observed to date ( $L_{\text{peak,bol}} = (2.2 \pm 0.2) \times 10^{45} \text{ erg s}^{-1}$ ). For comparison, the second brightest SLSN known, CSS100217 (Drake et al. 2011), was  $\sim 2$  times fainter at peak luminosity. Over an observed period of 108 d, ASASSN-15lh radiated  $\sim 1.1 \times 10^{52}$  erg of energy.

ASASSN-15lh was followed-up spectroscopically and showed blue continua with steep spectral slopes, lack of H or He and presence of broad O II ( $\lambda \simeq 4100 \text{ \AA}$ ) absorption features, justifying a SLSN-I classification. In retrospect, unlike other SLSN-I like SN 2010gx (Chomiuk et al. 2011) and PTF10cwr (Quimby et al. 2011), ASASSN-15lh lacks the broad O II feature at  $\lambda \simeq 4400 \text{ \AA}$  and appears to have a much brighter host galaxy than is typical (Leloudas et al. 2015; Dong et al. 2016). Black-body fits to the spectra yield a temperature evolution from  $\sim 21,000$  K around peak luminosity down to  $\sim 13,000$  K at later times ( $\sim 80$  d post peak light at rest-frame) and radii  $\sim 1 - 6 \times 10^{15}$  cm. Fits to the broad absorption features indicate SN ejecta expansion velocities of  $\sim 10,000 \text{ km s}^{-1}$ .

### 2.2. The late-time UV-bright plateau.

The bolometric light curve (LC) of ASASSN-15lh analyzed in this study, was assembled in the following way. The first part, covering the main peak and the subsequent decline to  $\sim 90$  days after explosion, was adopted from the bolometric luminosity curve as derived by Dong et al. (2016) (see their Table S2). For the second part, we downloaded the publicly available *Swift*/UVOT data (PI Brown, Holoinen, Quimby, Dong) and performed photometry using the standard *HEASOFT*<sup>2</sup> routines, similar to Dong et al. (2016). This resulted in the spectral energy distribution (SED) of the transient in *uvw2*, *uvm2*, *uvw1*, *u*, *b* and *v* bands extending up to  $\sim 200$  days after explosion.

After correcting the fluxes for Milky Way extinction and removing the contribution of the host galaxy, as described by Dong et al. (2016), we integrated the corrected SEDs against wavelength between the *Swift* *uvw2* and *v* bands (from  $\sim 2030 \text{ \AA}$  to  $5470 \text{ \AA}$ ). The missing fluxes at certain wavelengths and epochs were treated by linear interpolation between the neighboring flux values. The contribution from the unobserved red and infrared bands were approximated by matching a Rayleigh-Jeans tail at the *v*-band fluxes, and integrating this analytic curve between  $5470 \text{ \AA}$  and infinity. This rather crude approximation may be acceptable only for blue SEDs, that is, if the transient is hot. According to Dong et al. (2016), the color temperature of SN 2015L remained above  $10,000$  K by  $\sim 100$  days after explosion, which may suggest that the hot blackbody approximation does not cause large errors in the estimated bolometric fluxes at later epochs.

Finally, the resulting integrated LC was multiplied by a constant scaling factor in order to match the overlapping part with that of the luminosity curve by Dong et al. (2016). A very good match between the two datasets was found. The only notable difference is the appearance of the late-phase plateau, due to the re-brightening of the transient in the *UV* bands after  $\sim 100$  days (Brown et al. 2016; Margutti 2015).

Figure 1 shows the bolometric LC of ASASSN-15lh for the first  $\sim 220$  d in the rest-frame. Following Dong et al. (2016) we show two versions for the early LC: one corresponding to spectral energy distribution (SED) fitting assuming flat (solid black curve with filled circles) and one linear (dotted curve) temperature evolution. The red curve and filled circles show the bolometric late-time plateau obtained by SED fitting of data from the *Swift* UVOT (*uvw2* filter) through the *V*-band and a black-body tail attached for wavelengths longer than that.

We note that the early (first  $\sim 100$  d) part of the LC is nearly symmetric. Following the Nicholl et al. (2015) definitions of characteristic rise and decline timescales ( $t_{\text{rise}}$ ,  $t_{\text{dec}}$ ), the times before and after peak when the luminosity drops to  $L_{\text{peak}}/e$ , we find  $t_{\text{rise}} = 26.6$  d and  $t_{\text{dec}} = 29.3$  d indicating a nearly symmetric LC for the event, reminiscent of that for SLSN-I SCP06F6 (Barbary et al. 2009; Chatzopoulos et al. 2009; Quimby et al. 2011). These values place ASASSN-15lh significantly below the characteristic  $t_{\text{rise}}$  versus  $t_{\text{dec}}$  relation presented by Nicholl et al. (2015) and not correlated with the family of power-input models explored therein. The plateau phase ( $t > 90$  d) lasts for  $> 100$  d and is dominated by UV emission while the optical light shows a significant decline then. Therefore, any complete LC models explored for ASASSN-15lh need to account for both phases and be consistent with the emission properties observed in all corre-

<sup>2</sup> <http://heasarc.nasa.gov/heasoft/>

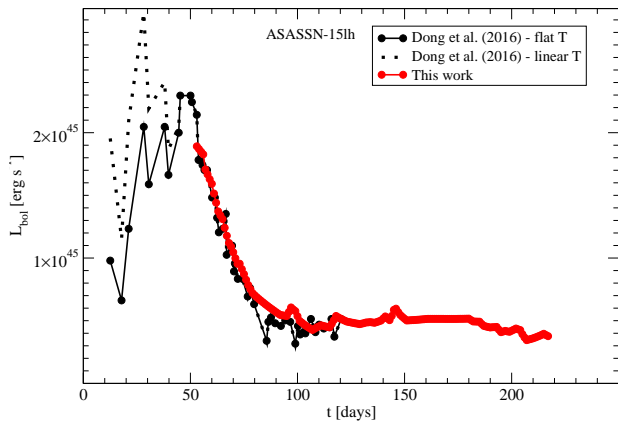


**Figure 1.** Extended observed bolometric light-curve of ASASSN-15lh. The three data sets shown correspond to SED fitting with a flat (solid black curve and black filled circles), and a linear (dotted curve) temperature at early times (Dong et al. 2016) and SED fitting of *Swift* UVOT and optical data during the late-phase plateau (this work; solid red curve and red filled circles).

sponding epochs.

### 2.3. The origin of ASASSN-15lh.

The extreme lightcurve of ASASSN-15lh has challenged all the power-input models discussed in the context of SNe and SLSNe (Dong et al. 2016). A purely radioactively powered LC would require  $> 30 M_{\odot}$  of  $^{56}\text{Ni}$  (Dong et al. 2016) while others estimate values as exotic as  $\sim 1500 M_{\odot}$  (Kozyreva et al. 2016). These calculations would imply an extremely massive progenitor star ( $M \gg 300 M_{\odot}$ ) that might directly collapse to a black hole and avoid a PISN explosion (Heger & Woosley 2002). Therefore we consider any pure  $^{56}\text{Ni}$ -power inputs very unlikely for ASASSN-15lh.

Magneto-rotational energy injection by a young magnetar has been discussed as the most likely power-input for ASASSN-15lh, assuming it was a SLSN but the implied magnetar parameters needed are extreme. Dong et al. (2016) estimate that, to match the observed peak bolometric luminosity of the event, a magnetar would need to have a magnetic field  $B_{\text{mag}} \simeq 10^{14}$  G and initial period  $P_{\text{mag}} = 1$  ms for 100% effective thermalization of the magnetar synchrotron radiation in the SN ejecta, an assumption that is debated by some authors<sup>3</sup> (Bucciantini et al. 2006). Yet another challenge to the magnetar model is presented by the fact that the SN ejecta will become transparent at late ( $> 100$  d) phases. At this stage, the magnetar-driven shock will be in radiative mode and therefore with an ever-decreasing velocity. The transition to this radiative loss regime is expected to lead to a short flash rather than a long, bright plateau phase as observed for ASASSN-15lh. The efficiency of the magnetar model in powering superluminous events has been recently challenged by some authors who find that increasing magnetar input energy gets converted to kinetic energy rather than luminosity (Wang et al. 2016). Others (Metzger et al. 2015; Sukhbold & Woosley 2016; Bersten et al. 2016) also favor a magnetar scenario but derive somewhat different param-

eters ( $B_{\text{mag}} = 1.2 \times 10^{13}$  G,  $P_{\text{mag}} = 1.2$  ms and SN ejecta mass  $M_{\text{SN}} = 3.0 M_{\odot}$ ,  $B_{\text{mag}} = 4 \times 10^{13}$  G,  $P_{\text{mag}} = 0.7$  ms,  $M_{\text{SN}} = 3.4 M_{\odot}$  and  $B_{\text{mag}} = (0.3 - 1) \times 10^{14}$  G,  $P_{\text{mag}} = 1-2$  ms,  $M_{\text{SN}} = 6.0 M_{\odot}$  respectively). A principal caveat of these models is that they were fit to the first  $\sim 100-150$  d of the ASASSN-15lh, before the later, UV-bright long plateau phase. Therefore the predicted long-term decline from a magnetar-powered LC fails to capture the late behavior of the event. In addition, magnetar radiation has difficulty accounting for the strong UV emission during the plateau, assuming that the radiation is thermalized and re-processed to longer (optical, infrared) wavelengths. Although some simple radiation transfer models involving magnetar input have been discussed in the literature (Dessart et al. 2012), more numerical work is needed to model the spectral properties of SLSN-I powered by this mechanism and explore how well it reproduces the observed spectra of these events in contemporaneous epochs.

The absence of circumstellar emission features in the spectra is often presented as evidence against a CSM interaction-powered SLSN scenario for SLSN-I but can, in principle, fit the LCs of all SLSNe and account for their observed diversity (Chatzopoulos et al. 2013a,b). Nevertheless, calculating the radiative properties and spectral line emission from the dense shells bounded by a forward and a reverse shock following CSM interaction is a challenge for conventional spectral synthesis and radiation transfer codes (Dessart et al. 2015, 2016). This is due to a variety of reasons. First, the bulk of the emission is produced in a narrow region where the velocity profile departs from a monotonic homologous profile, an assumption inherent to SN radiation transfer codes. Second, the ionization and recombination properties of elements other than H and He are very sensitive to the local conditions of temperature and density and, at high temperatures ( $\sim 21,000$  K for ASASSN-15lh), recombination from intermediate mass elements like oxygen, carbon and magnesium may be strained, leading to suppression of line emission. As is the case of magnetar spin-down models, more simulations and non-local thermal equilibrium (LTE) radiation transfer calculations of H-poor CSM interaction are needed across the relevant parameter space to fully assess the relevance of this model to SLSN-I.

The possibility of a tidal disruption event (TDE), involving a star disrupted by a supermassive black hole, cannot be excluded given the fact that the position of ASASSN-15lh is astrometrically consistent with the center of its host galaxy. Some issues with this interpretation are the lack of H/He lines in the spectra, the temperature evolution of the event, which is inconsistent with other TDE candidates (Dong et al. 2016), and the fact that the very massive, old host of the event would require a central supermassive black hole with mass far above the ones calculated for TDE models consistent with other luminous transients (Vinkó et al. 2015; Yoon et al. 2015).

Alternative interpretations of ASASSN-15lh, not involving a SN explosion, have also been discussed yet so far rejected (Dong et al. 2016). These include amplification of a lower luminosity event due to gravitational lensing or active galactic nuclei (AGN) radiation. Finally, more exotic scenarios proposed for ASASSN-15lh include birth of a rapidly rotating strange quark star (Dai et al. 2016) and jet energy input by a rapidly rotating magnetar (Gilkis et al. 2015; Soker 2016).

In the following paragraph we explore ASASSN-15lh as an extreme SLSN powered by a combination of luminosity inputs capable of reproducing both the early bright phase and

<sup>3</sup> [http://wwwmpa.mpa-garching.mpg.de/hydro/NucAstro/PDF\\_16/Badjin.pdf](http://wwwmpa.mpa-garching.mpg.de/hydro/NucAstro/PDF_16/Badjin.pdf)

the late-time plateau of the transient.

### 3. EXTREME SUPERNOVA MODELS FOR ASASSN-15lh

To fit the full LC of ASASSN-15lh including the late-time, UV-bright plateau phase, we have updated the semi-analytical models of (Chatzopoulos et al. 2012, 2013b) to include contributions from all three power-input mechanisms: gamma-ray heating by the radioactive decays of  $^{56}\text{Ni}$  and  $^{56}\text{Co}$ , magnetar spin-down and forward and reverse shock heating following CSM interaction. A C++ code was developed to integrate the combined input over the SN ejecta and CSM mass where appropriate, following the prescriptions of (Arnett 1980, 1982). These semi-analytic models were designed to allow the rapid and efficient exploration of a large range of multiple parameters when nature takes us to uncharted territory. ASASSN-15lh presents an ideal case to employ these tools.

Model fits to the observed LC of ASASSN-15lh were computed using best-fitting techniques to yield the following parameters: mass of  $^{56}\text{Ni}$  ( $M_{\text{Ni}}$ ), magnetic field and initial period of newly-formed magnetar ( $B_{\text{mag}}$ ,  $P_{\text{mag}}$  and consequently, magnetar spin-down time-scale  $t_p$ ), SN ejecta and CSM mass ( $M_{\text{SN}}$ ,  $M_{\text{CSM}}$ ), velocity of SN ejecta ( $v_{\text{SN}}$ ), power-law slope of CSM density ( $s$ , a value of 0 represents a shell and a value of 2 a steady-state radiatively-driven wind), implied pre-SN mass-loss rate ( $\dot{M}$ ) and CSM density and distance from the progenitor ( $\rho_{\text{CSM}}$ ,  $R_{\text{CSM}}$ ). For all cases explored here for ASASSN-15lh, the contribution of the radioactive decay of  $^{56}\text{Ni}$  was negligible even for up to  $\sim 6 M_{\odot}$  expected for some massive, energetic core-collapse SNe (Umeda & Nomoto 2008). Since physically plausible full-fledged PISNe models able to produce higher  $^{56}\text{Ni}$  yields cannot reproduce the LC of ASASSN-15lh, we do not consider the contribution from this input in our final fits.

A combined CSM interaction and magnetar input model has been proposed for the superluminous SN 2015bn (Nicholl et al. 2016). Their estimates suggest that the early, bright portion of the LC of SN 2015bn is powered mainly by magnetar spin-down while the late-time optical luminosity arises through continued CSM interaction with a dense, extended wind. In addition, SN 2015bn exhibited undulations in its LC that may be indicative of different heating mechanisms or variations in the CSM density. Similar arguments may account for the variations seen in the late-time ( $t > 100$  d) LC of ASASSN-15lh.

In the present work, we explore two categories of LC models: hybrid CSM interaction and magnetar spin-down models (labeled CSM0\_A, CSM0\_B, CSM2\_A, CSM2\_B) and pure CSM interaction models including interaction due to PPISN events (labeled CSM0, CSM2). We consider CSM interaction for the cases of a dense shell ( $s = 0$ ; CSM0\_A, CSM0\_B and CSM0 models) and a wind ( $s = 2$ ; CSM2\_A, CSM2\_B and CSM2 models). We also explore the relative contributions of the two inputs for both the early, bright-peak phase and the late-time plateau of ASASSN-15lh. The final fitting parameters for all six models are presented in Table 1 and the fits to the observed LC of ASASSN-15lh are shown in Figure 2. In Figure 2, we also plot the individual contributions to the total luminosity by the magnetar spin-down input ( $L_{\text{mag}}$ ), and the forward ( $L_{\text{CSM,f}}$ ) and reverse ( $L_{\text{CSM,r}}$ ) shock heating due to the CSM interaction.

#### 3.1. Combined Circumstellar Interaction and Magnetar Spin-down Input.

We first consider models that involve both magnetar spin-down and CSM interaction contributions to the final luminosity. The top four panels of Figure 2 show our best-fits to the LC of ASASSN-15lh. In these cases, the ‘‘A’’ models invoke the magnetar energy as the main source of the late-time plateau phase while CSM interaction dominates the early bright part of the LC. The ‘‘B’’ models on the other hand, include strong contributions from both power inputs to reproduce the early part of the LC while the plateau phase is dominated by reverse shock heating due to CSM interaction.

We were unable to reproduce the late-time plateau with a combined magnetar/CSM interaction model that involves a dense CSM wind (model CSM2\_B). For a reasonable combination of parameters, the reverse shock luminosity declines very rapidly at late times and has little contribution to the total output.

On the other hand, CSM interaction with a  $\sim 19 M_{\odot}$  dense shell ( $s = 0$ ; model CSM0\_B) enhances the relative contribution of the reverse shock to levels that can reproduce a plateau for  $t > 100$  d. We find that, to reproduce the main, bright peak of ASASSN-15lh, a magnetar with  $B_{\text{mag}} \simeq 10^{14}$  G and  $P_{\text{mag}} \simeq 1$  ms is required, consistent with the findings of Bersten et al. (2016). Assuming H-poor material (opacity  $\kappa = 0.2 \text{ cm}^2 \text{ g}^{-1}$ ), however, we derive a much higher SN ejecta mass ( $M_{\text{SN}} = 36 M_{\odot}$ ). Part of our disagreement on the SN ejecta mass is the fact that it affects the CSM interaction contributions in our hybrid model and the ratio of the luminosity supplied by the forward and the reverse shocks. The late-time plateau luminosity is provided by the continuous CSM interaction and more specifically by reverse shock heating. Radiative shock heating is also consistent with the observation that the bulk of the plateau luminosity is in UV wavelengths. The shell mass and implied mass-loss rate ( $\dot{M} = 1.2 M_{\odot} \text{ yr}^{-1}$ ) suggest a CSM shell density of  $\sim 1.7 \times 10^{-14} \text{ g cm}^{-3}$  at a radius of  $6 \times 10^{15}$  cm, that is consistent with the black body radii calculated by Dong et al. (2016).

The combined SN ejecta and CSM shell mass ( $\simeq 55 M_{\odot}$ ) for model CSM0\_B implies an extreme progenitor that may be consistent with a rapidly-rotating pulsational PISN (PPISN; Chatzopoulos & Wheeler 2012b) or a Luminous Blue Variable (LBV; Smith & Owocki 2006). It has been shown that rotationally-induced mixing including the effects of the magnetic fields (via the Spruit-Taylor dynamo mechanism; Spruit 1999, 2002) can lead to H and He deficient, bare carbon-oxygen (CO) cores by the onset of PPISN and ejection of massive H-poor shells by that process (Chatzopoulos & Wheeler 2012a,b; Chatzopoulos et al. 2013a). Rapid progenitor rotation is also a requirement for the formation of a rapidly rotating magnetar to supply the additional luminosity needed to fit the early, bright phase LC of ASASSN-15lh. This model requires the energetic ( $\sim 4 \times 10^{52}$  erg) core-collapse of a massive CO core within a previously ejected H-poor shell via PPISN inevitably leading to H-deficient CSM interaction.

One caveat of this interpretation is the requirement of large explosion energy, well above the characteristic  $\sim 10^{51}$  erg kinetic energy for conventional SNe. Nevertheless, for an event as unique as ASASSN-15lh that is not impossible (Umeda & Nomoto 2008). In addition, it is possible to tap a fraction of the magnetar spin-down rotational energy to enhance SN ejecta kinetic energy and the final SN explosion (Wheeler

**Table 1**  
Fitting and derived parameters for the LC models of ASASSN–15lh presented in this work.

Parameter	CSM0_A	CSM0_B	CSM2_A	CSM2_B	CSM0	CSM2
<b>Magnetar spin-down</b>						
$B_{\text{mag}}$ ( $10^{14}$ G)	0.12	1.09	0.11	1.09	–	–
$P_{\text{mag}}$ (ms)	1.00	1.58	1.00	1.58	–	–
$t_p$ (days)	330	10	392	10	–	–
<b>Circumstellar Interaction</b>						
$M_{\text{SN}}$ ( $M_{\odot}$ )	6.00	36.00	33.00	10.00	36.00	35.00
$v_{\text{SN}}$ ( $10^4$ km s $^{-1}$ ) <sup>†</sup>	5.95	3.61	3.36	3.34	3.60	3.26
$E_{\text{SN}}$ (foe)	16.0	42.0	40.0	12.0	50.0	40.0
$s$	0	0	2	2	0	2
$M_{\text{CSM}}$ ( $M_{\odot}$ )	22.00	19.00	19.00	20.00	19.50	20.00
$\dot{M}$ ( $M_{\odot}$ yr $^{-1}$ )	0.45	0.20	0.80	1.20	0.20	1.20
$\rho_{\text{CSM}}$ ( $10^{-15}$ g cm $^{-3}$ )	2.79	1.57	11.16	16.74	4.02	37.66
$R_{\text{CSM}}$ ( $10^{15}$ cm)	9.00	8.00	6.00	6.00	5.00	4.00

**Note.** — <sup>†</sup> The SN ejecta velocity is related to the SN energy via the expression  $v_{\text{SN}} = [10(n-5)E_{\text{SN}}/3(n-3)M_{\text{SN}}]^{0.5}$  where  $n$  is the power-law index for the density of the outer SN ejecta (Chevalier & Fransson 1994).

et al. 2000; Kasen & Bildsten 2010). At high degrees of pre-SN rotation, the formation of energetic jets is also a possibility and a collapsar-like, collimated explosion, similar to that considered for GRBs, is possible. In such case, we expect the SN ejecta and the subsequent interaction to be asymmetric (Couch et al. 2009).

Yet another concern is the challenge to form a massive ( $\sim 60 M_{\odot}$  at Zero Age Main Sequence (ZAMS)) star in a host galaxy with such low observed SFR and high metallicity that is considerably different than many of other SLSN hosts (Lunnan et al. 2014). However, the SFR in the galactic center, which is consistent with the location of ASASSN–15lh, may be significantly different from the bulk of the galaxy (as is the case for the Milky Way). Another scenario is the possibility of forming a massive star through stellar dynamical processes (mergers, captures and collisions) in dense nuclear star clusters (Bonnell & Bate 2005).

Another issue is the need to form a magnetar, instead of a black hole, for such a massive CCSN progenitor (Heger & Woosley 2002). We note, however, that the core mass limits to form a pulsar versus a black hole with the inclusion of magneto-rotational effects are still debated making proto-magnetar formation hard, but not impossible (Ugliano et al. 2012; Sukhbold & Woosley 2014; Mösta et al. 2014, 2015). Likewise, it is not known what evolution leads to “normal” pulsars, what to highly-magnetized magnetars, and what to compact central objects as observed in Cas A. Some magnetars may arise from especially high-mass stars that are otherwise thought to perhaps foster black hole formation (Muno et al. 2006). In addition, for rapid enough rotation the fissioning of the collapsed remnants of stars is possible and may lead to the formation of black hole or black hole – neutron star binaries (Reisswig et al. 2013; Woosley 2016). Although it is unknown whether or not this mechanism can efficiently lead to magnetar fragments, it is a possibility worth mentioning.

The late-time plateau phase of ASASSN–15lh can also be successfully reproduced by models where the magnetar energy input dominates in later times (CSM0\_A and CSM2\_A). For these models, the bulk of the early, bright LC is powered by CSM interaction (mainly forward shock heating). Our fit for a model involving interaction with a steady-state wind (CSM2\_A) is better than that with a shell (CSM0\_A), but given the assumptions and limitations of the analytical mod-

els we cannot distinguish between the two. For both of these models, we derive magnetar parameters that are consistent with those of Metzger et al. (2015) and Sukhbold & Woosley (2016) ( $B_{\text{mag}} = (1.1-1.2) \times 10^{13}$  G and  $P_{\text{mag}} = 1$  ms). Both models require interaction with a massive H-poor shell similar in model CSM0\_B ( $M_{\text{CSM}} = 19-22 M_{\odot}$ ). One difference is that a much smaller  $M_{\text{SN}}$  is derived for model CSM0\_A ( $M_{\text{SN}} = 6 M_{\odot}$ ) compared to model CSM2\_A. This is due to the fact that, for model CSM0\_A, the reverse shock input truncates at  $t \simeq 75$  d in order to allow for the magnetar spin-down tail to supply the luminosity deficit to power the late-phase plateau. As a result, model CSM0\_A implies the SN explosion from a Type Ic CCSN (progenitor mass  $\sim 12-15 M_{\odot}$ ) within a massive H-poor shell. The main issue of this model is that large SN ejecta kinetic energy ( $E_{\text{SN}} \sim 6 \times 10^{51}$  erg) is still required to account for the bright peak of ASASSN–15lh powered by comparable amounts of the two inputs implying high-velocity SN ejecta. It must be mentioned that, as discussed in § 3.1, it is hard to attain efficient magnetar radiation in late times. In addition, many of the implied magnetar spin-down time-scales ( $t_p$  values in Table 1) are considerably longer than those predicted (Thompson et al. 2004). These are strong counter-arguments against long-duration magnetar energy input for ASASSN–15lh.

Model CSM2\_A also provides a good fit to the observed LC but requires  $M_{\text{SN}}$  and  $M_{\text{CSM}}$  that are closer to model CSM0\_B. A problem with this model is the origin of such a high-mass ( $22 M_{\odot}$ ) steady-state wind around the progenitor star (derived mass-loss rate  $\dot{M} = 0.8 M_{\odot}$  yr $^{-1}$ ). This yields  $M_{\text{CSM}}/\dot{M} \sim 24$  years of wind mass-loss prior to the SN explosion implying that it might have started during the late, core oxygen burning phase of the SN. The possibility of the existence of a close binary companion can alter this result. In addition, provided that the host of ASASSN–15lh is a regular, near-solar metallicity galaxy, it is possible that high wind mass-loss rates are encountered for massive rapidly rotating stars in this environment. Another open question with regards to models CSM0\_A and CSM2\_A remains the UV-bright nature of the plateau luminosity and whether radiation from the spin-down of a young magnetar can account for it.

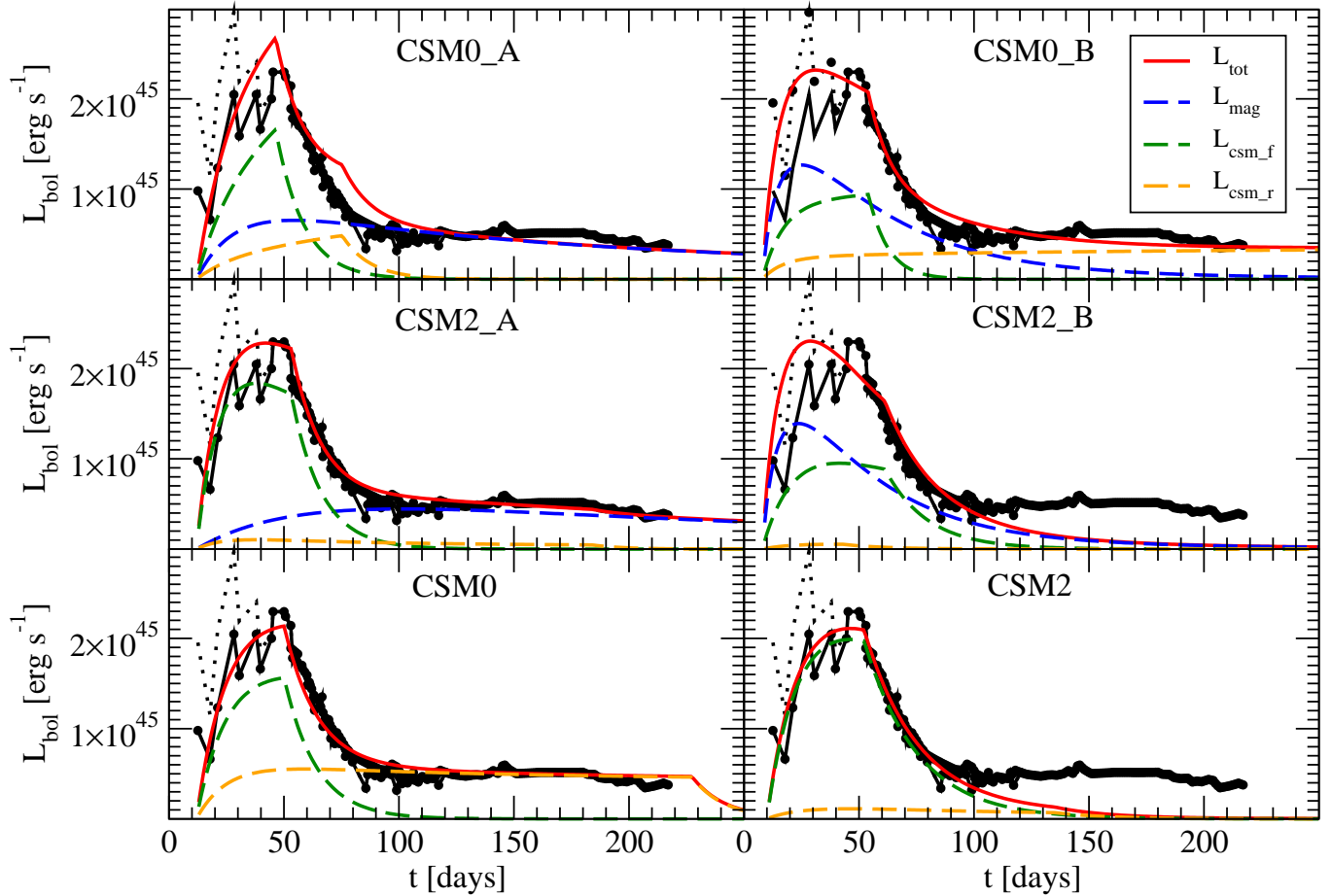


**Figure 2.** Fits to the observed bolometric light–curve of ASASSN–15lh (filled circles and solid black curve). The dotted curve shows the bolometric luminosity of ASASSN–15lh during the rise to peak derived from SED fitting with a linear temperature at early time following [Dong et al. \(2016\)](#). Total combined model luminosity ( $L_{\text{tot}}$ ) is shown in solid red curves and individual contributions by magnetar spin–down energy injection ( $L_{\text{mag}}$ ), forward ( $L_{\text{csm,f}}$ ) and reverse ( $L_{\text{csm,r}}$ ) shock heating are shown in dashed blue, green and orange curves respectively. The fitting parameters for all models are given in Table 1.

### 3.2. Pulsational PISN and Hydrogen–Poor CSM Interaction.

Another possibility for ASASSN–15lh is a pure H–poor CSM interaction scenario involving the collision of massive shells ejected by a PPISN ([Woosley et al. 2007](#); [Chatzopoulos & Wheeler 2012b](#); [Sukhbold & Woosley 2016](#)). A problem with a pure PPISN shell collision scenario is the implied energetics; simulations of PPISNe yield kinetic energies of the order of  $10^{51}$  erg for the shells over time–scales of months to a year implying luminosities up to  $\sim 10^{44}$  erg  $\text{s}^{-1}$  ([Woosley et al. 2007](#); [Sukhbold & Woosley 2016](#)). In light of these results, the only possibility would be interaction of massive SN ejecta by an energetic CCSN following the last PPISN shell ejection. The explosion would then form a few  $M_{\odot}$  of  $^{56}\text{Ni}$  and could leave a black hole behind but the bulk of the lu-

minosity would be provided by the forward and the reverse shocks following CSM interaction.

Models CSM0 and CSM2 in the lower two panels of Figure 2 show pure CSM interaction fits to the LC of ASASSN–15lh. As was the case for model CSM2\_B, model CSM2 fails to reproduce the late–time plateau leaving CSM0 as the only viable possibility thus suggesting interaction with a dense shell. For this model,  $36 M_{\odot}$  of H–poor SN ejecta interacts with an also H–poor  $19.5 M_{\odot}$  CSM for a total mass of  $\sim 55.5 M_{\odot}$  consistent with a rapidly–rotating PPISN progenitor. The derived  $\dot{M}$  of  $0.2 M_{\odot} \text{ yr}^{-1}$  suggest that the shell ejection occurred  $\sim 100$  years prior to the SN. This timescale is consistent with some of the timescales between PPISN pulses listed in Supplementary Table 1 of [Woosley et al. \(2007\)](#) for non–rotating progenitors in the mass range

54–56  $M_{\odot}$  in agreement with the parameters implied by the CSM0 model LC fit. The derived radius of the CSM shell ( $R_{\text{CSM}} = 5 \times 10^{15}$  cm) is also consistent with the black body fits presented by [Dong et al. \(2016\)](#).

One common objection to models of H-poor CSM interaction for SLSN-I is the absence of interaction features like those seen for SLSN-II (luminous SN IIn) events. We stress, however, that more numerical work and updated algorithms need to be implemented in non-LTE radiation transfer codes to carefully evaluate the conditions that allow emission line formation for elements other than H and He for non-homologous, non-monotonic velocity profiles ([Chatzopoulos et al. 2013b](#); [Dessart et al. 2015, 2016](#)).

#### 4. DISCUSSION AND CONCLUSIONS

In this paper we studied physically plausible SN models that may account for the LC of the record-breaking SLSN-I ASASSN-15lh (or SN 2015L; [Dong et al. 2016](#)). Our goal was to fit the complete LC of the event, including the latest ( $t > 100$  d) observations that show a UV-bright plateau phase suggesting continuous heating of the SN ejecta.

To that goal we employed semi-analytic “hybrid” models that consider the contribution of all three power-input mechanisms discussed for SLSNe: the radioactive decays of  $^{56}\text{Ni}$  and  $^{56}\text{Co}$ , energy injection by the spin-down of a newly born magnetar and CSM interaction. We found that in all plausible cases the contribution of  $^{56}\text{Ni}$  input is negligible, therefore we focused on models of magnetar spin-down and forward and reverse shock heating following H-poor CSM interaction. Also, we studied cases where the late-time plateau is powered either by the magnetar input or by reverse shock heating and discussed implications with regards to the observed UV-bright flux during this phase.

We found that models that involve interaction with a massive steady-state wind (CSM2\_B and CSM2) fail to reproduce the late plateau phase with the exception of model CSM2\_A where the magnetar input supplies the luminosity deficit for  $t > 80$  d.

On the contrary, models that invoke interaction with a massive dense shell lost via an eruptive mass-loss mechanism (CSM0\_A, CSM0\_B and CSM0) provide the best fits to the LC of ASASSN-15lh. Nevertheless, there are issues with the hybrid models invoking a magnetar input since it requires the presence of a magnetar and more fine-tuning to fit the LC of ASASSN-15lh. There are also yet unresolved issues with efficient thermalization of magnetar radiation in the SN ejecta and conversion to luminosity discussed in § 3.1. As such, the more consistent and better constrained single-input model CSM0 where the reverse shock provides the luminosity for the late-time plateau is favored in our analysis. The derived parameters from our fits suggest a common theme: interaction of massive SN ejecta ( $M_{\text{SN}} \simeq 36 M_{\odot}$  with a H-poor CSM shell of  $\sim 20 M_{\odot}$ ). The derived total SN ejecta and CSM masses of our models support a scenario where a rapidly-rotating energetic CCSNe exploded within a previously shed massive H-deficient shell ejected either via the PPISN ([Woosley et al. 2007](#)) or the LBV ([Smith & Owocki 2006](#)) mechanism. Schematic diagrams of the proposed alternative progenitor and power-input configurations for ASASSN-15lh are shown in Figure 3.

A rapidly rotating ( $> 50\%$  of the break-up speed at the equator)  $\sim 50$ - $60 M_{\odot}$  star may undergo enhanced mixing allowing it to reach the PPISN regime during its core oxygen burning phase ([Chatzopoulos et al. 2013a](#)). At this phase,

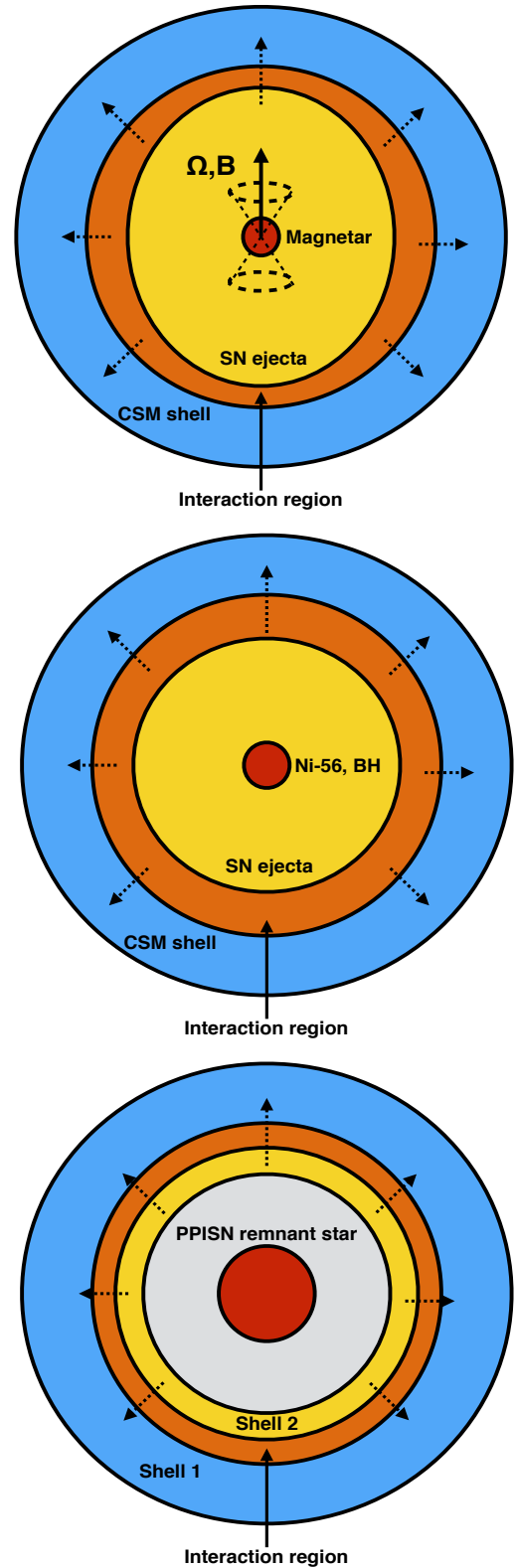


**Figure 3.** Schematic diagrams of three possible progenitor models for ASASSN-15lh. *Upper panel:* Massive, rapidly rotating CCSN explosion following shell ejection due to a PPISN. Radiative energy input is supplied by the spin-down of a newly-born magnetar in the center combined with H-poor CSM interaction of the SN ejecta with the PPISN shell. Rapid rotation is required for magnetar formation that can lead to asymmetric SN ejecta (§ 3). *Middle panel:* Interaction of H-poor SN ejecta from a massive CCSN following shell ejection due to a PPISN. The core of the progenitor star in this case collapses to a black-hole and produces  $\sim 1$ - $4 M_{\odot}$  of  $^{56}\text{Ni}$ . *Lower panel:* H-poor interaction between massive PPISN shells perhaps followed by an energetic SN explosion.

the star may have lost the entirety of its H and He envelope due to enhanced mass-loss because of rotation, duplicity or strong winds as expected for the host of ASASSN-15lh that is a bright, near-solar metallicity galaxy. Upon undergoing the PPISN, the bare CO core of the star can eject several solar masses of H-poor material forming a massive shell around the remnant. The core remnant can then evolve to become an energetic ( $\sim 10^{52}$  erg) CCSN explosion inevitably leading to strong CSM interaction.

The forward and reverse shock heat deposition in the H-poor CSM shell and SN ejecta could be supplemented by radiation from a newly-born rapidly-rotating magnetar ( $B_{\text{mag}} = (1.1 - 1.2) \times 10^{13}$  G and  $P_{\text{mag}} = 1$  ms). Upon the collapse of such massive progenitor, black hole formation may be more likely, but alternative channels exist to allow for magnetar birth (Muno et al. 2006; Ugliano et al. 2012; Sukhbold & Woosley 2014; Woosley 2016). The fact that the plateau phase is UV-bright, however, favors a shock heating input for the late luminosity of ASASSN-15lh consistent with a single-input strong CSM interaction scheme.

Current and next generation transient searches like the Zwicky Transient Factory (ZTF), PanSTARRS and LSST will likely yield more extraordinary events like ASASSN-15lh that put the known SN power engine models to the test. In addition, radio observations of SLSN-I may help distinguish between the different power-input mechanisms (Nicholl et al. 2016). In tandem, advances in numerical algorithms and parallel computing will eventually allow us to accurately model the spectra of SLSN-I and be a step closer to understanding the extreme origins of extreme supernovae.

The research of EC and JCW is supported by NASA grant HST-AR-13276.002-A. EC thanks the Enrico Fermi Institute for its support via the Enrico Fermi Fellowship.

## REFERENCES

- Arnett, W. D. 1980, *ApJ*, 237, 541  
 —. 1982, *ApJ*, 253, 785  
 Barbary, K. et al. 2009, *ApJ*, 690, 1358, 0809.1648  
 Bersten, M. C., Benvenuto, O. G., Orellana, M., & Nomoto, K. 2016, *ApJL*, 817, L8, 1601.01021  
 Bonnell, I. A., & Bate, M. R. 2005, *MNRAS*, 362, 915, astro-ph/0506689  
 Brown, P. J. et al. 2016, *ArXiv e-prints*, 1605.03951  
 Bucciantini, N., Thompson, T. A., Arons, J., Quataert, E., & Del Zanna, L. 2006, *MNRAS*, 368, 1717, astro-ph/0602475  
 Chatzopoulos, E., van Rossum, D. R., Craig, W. J., Whalen, D. J., Smidt, J., & Wiggins, B. 2015, *ApJ*, 799, 18, 1410.0039  
 Chatzopoulos, E., & Wheeler, J. C. 2012a, *ApJ*, 748, 42, 1201.1328  
 —. 2012b, *ApJ*, 760, 154, 1210.1617  
 Chatzopoulos, E., Wheeler, J. C., & Couch, S. M. 2013a, *ApJ*, 776, 129, 1308.4660  
 Chatzopoulos, E., Wheeler, J. C., & Vinko, J. 2009, *ApJ*, 704, 1251, 0909.1798  
 —. 2012, *ApJ*, 746, 121, 1111.5237  
 Chatzopoulos, E., Wheeler, J. C., Vinko, J., Horvath, Z. L., & Nagy, A. 2013b, *ApJ*, 773, 76, 1306.3447  
 Chatzopoulos, E. et al. 2011, *ApJ*, 729, 143, 1101.3581  
 Chevalier, R. A., & Fransson, C. 1994, *ApJ*, 420, 268  
 Chomiuk, L. et al. 2011, *ApJ*, 743, 114, 1107.3552  
 Couch, S. M., Wheeler, J. C., & Milosavljević, M. 2009, *ApJ*, 696, 953, 0812.3918  
 Dai, Z. G., Wang, S. Q., Wang, J. S., Wang, L. J., & Yu, Y. W. 2016, *ApJ*, 817, 132, 1508.07745  
 Dessart, L., Audit, E., & Hillier, D. J. 2015, *MNRAS*, 449, 4304, 1503.05463  
 Dessart, L., Hillier, D. J., Audit, E., Livne, E., & Waldman, R. 2016, *MNRAS*, 1602.02977  
 Dessart, L., Hillier, D. J., Waldman, R., Livne, E., & Blondin, S. 2012, *MNRAS*, 426, L76, 1208.1214  
 Dessart, L., Waldman, R., Livne, E., Hillier, D. J., & Blondin, S. 2013, *MNRAS*, 428, 3227, 1210.6163  
 Dong, S. et al. 2016, *Science*, 351, 257, 1507.03010  
 Drake, A. J. et al. 2011, *ApJ*, 735, 106, 1103.5514  
 Gal-Yam, A. 2012, *Science*, 337, 927, 1208.3217  
 Gal-Yam, A. et al. 2009, *Nature*, 462, 624, 1001.1156  
 Gilkis, A., Soker, N., & Papish, O. 2015, *ArXiv e-prints*, 1511.01471  
 Grasberg, E. K., & Nadezhin, D. K. 1986, *Soviet Astronomy Letters*, 12, 68  
 Heger, A., & Woosley, S. E. 2002, *ApJ*, 567, 532, astro-ph/0107037  
 Inserra, C. et al. 2013, *ApJ*, 770, 128, 1304.3320  
 Kasen, D., & Bildsten, L. 2010, *ApJ*, 717, 245, 0911.0680  
 Kasen, D., Woosley, S. E., & Heger, A. 2011, *ApJ*, 734, 102, 1101.3336  
 Kozyreva, A., & Blinnikov, S. 2015, *MNRAS*, 454, 4357, 1510.00439  
 Kozyreva, A., Blinnikov, S., Langer, N., & Yoon, S.-C. 2014a, *A&A*, 565, A70, 1403.5212  
 Kozyreva, A., Hirschi, R., Blinnikov, S., & den Hartogh, J. 2016, *ArXiv e-prints*, 1603.00335  
 Kozyreva, A., Yoon, S.-C., & Langer, N. 2014b, *A&A*, 566, A146, 1405.6340  
 Leloudas, G. et al. 2015, *MNRAS*, 449, 917, 1409.8331  
 Lunnan, R. et al. 2014, *ApJ*, 787, 138, 1311.0026  
 Margutti, R. 2015, *The Astronomer's Telegram*, 8089  
 Metzger, B. D., Margalit, B., Kasen, D., & Quataert, E. 2015, *MNRAS*, 454, 3311, 1508.02712  
 Moriya, T. J., Blinnikov, S. I., Tominaga, N., Yoshida, N., Tanaka, M., Maeda, K., & Nomoto, K. 2013, *MNRAS*, 428, 1020, 1204.6109  
 Moriya, T. J., & Tominaga, N. 2012, *ApJ*, 747, 118, 1110.3807  
 Mösta, P., Ott, C. D., Radice, D., Roberts, L. F., Schnetter, E., & Haas, R. 2015, *Nature*, 528, 376, 1512.00838  
 Mösta, P. et al. 2014, *ApJL*, 785, L29, 1403.1230  
 Muno, M. P. et al. 2006, *ApJL*, 636, L41, astro-ph/0509408  
 Neill, J. D. et al. 2011, *ApJ*, 727, 15, 1011.3512  
 Nicholl, M. et al. 2016, *ArXiv e-prints*, 1603.04748  
 —. 2014, *MNRAS*, 444, 2096, 1405.1325  
 —. 2015, *MNRAS*, 452, 3869, 1503.03310  
 Nomoto, K., Tominaga, N., Tanaka, M., Maeda, K., & Umeda, H. 2007, in *American Institute of Physics Conference Series*, Vol. 937, *Supernova 1987A: 20 Years After: Supernovae and Gamma-Ray Bursters*, ed. S. Immler, K. Weiler, & R. McCray, 412–426, 0707.2187  
 Ostriker, J. P., Spitzer, Jr., L., & Chevalier, R. A. 1972, *ApJL*, 176, L51  
 Planck Collaboration et al. 2014, *A&A*, 571, A16, 1303.5076  
 Quimby, R. M., Aldering, G., Wheeler, J. C., Höflich, P., Akerlof, C. W., & Rykoff, E. S. 2007, *ApJL*, 668, L99, 0709.0302  
 Quimby, R. M. et al. 2011, *Nature*, 474, 487, 0910.0059  
 Reisswig, C., Ott, C. D., Abdikamalov, E., Haas, R., Mösta, P., & Schnetter, E. 2013, *Physical Review Letters*, 111, 151101, 1304.7787  
 Shappee, B. J. et al. 2014, *ApJ*, 788, 48, 1310.2241  
 Shklovskii, I. S. 1976, *Soviet Ast.*, 19, 554  
 Smith, N. et al. 2007, *ApJ*, 666, 1116, astro-ph/0612617  
 Smith, N., & McCray, R. 2007, *ApJL*, 671, L17, 0710.3428  
 Smith, N., & Owocki, S. P. 2006, *ApJL*, 645, L45, astro-ph/0606174  
 Soker, N. 2016, *ArXiv e-prints*, 1602.07343  
 Spruit, H. C. 1999, *A&A*, 349, 189, astro-ph/9907138  
 —. 2002, *A&A*, 381, 923, astro-ph/0108207  
 Sukhbold, T., & Woosley, S. 2016, *ArXiv e-prints*, 1602.04865  
 Sukhbold, T., & Woosley, S. E. 2014, *ApJ*, 783, 10, 1311.6546  
 Thompson, T. A., Chang, P., & Quataert, E. 2004, *ApJ*, 611, 380, astro-ph/0401555  
 Ugliano, M., Janka, H.-T., Marek, A., & Arcones, A. 2012, *ApJ*, 757, 69, 1205.3657  
 Umeda, H., & Nomoto, K. 2008, *ApJ*, 673, 1014, 0707.2598  
 Vinkó, J. et al. 2015, *ApJ*, 798, 12, 1410.6014  
 Wang, L.-J., Wang, S. Q., Dai, Z. G., Xu, D., Han, Y.-H., Wu, X. F., & Wei, J.-Y. 2016, *ApJ*, 821, 22, 1602.06190  
 Wheeler, J. C., Yi, I., Höflich, P., & Wang, L. 2000, *ApJ*, 537, 810, astro-ph/9909293  
 Woosley, S. E. 2010, *ApJL*, 719, L204, 0911.0698  
 —. 2016, *ArXiv e-prints*, 1603.00511  
 Woosley, S. E., Blinnikov, S., & Heger, A. 2007, *Nature*, 450, 390, 0710.3314  
 Yoon, Y. et al. 2015, *ApJ*, 808, 96, 1507.08843